An *In-Situ* Scanning Electron Microscopy Study of the Bonding between MnS Inclusions and the Matrix during Tensile Deformation of Hot-Rolled Steels

S. B. HOSSEINI, C. TEMMEL, B. KARLSSON, and N.-G. INGESTEN

The bonding between manganese sulfide (MnS) inclusions and the surrounding steel matrix was investigated by *in-situ* tensile testing in a scanning electron microscope (SEM) at room temperature. Tests were carried out for two different orientations of the inclusions with respect to the loading axis. The orientation was created during a hot cross rolling operation of the test material. Straining was performed along both longitudinal (L) and short transverse (S) directions. The investigation showed that the bond between the MnS inclusions and the matrix is weak. This was particularly seen in the S test direction where the sulfides, lying perpendicular to the load axis, delaminated from the matrix at very low applied stresses. The MnS inclusions in longitudinal tests instead fractured at high stress levels close to the yield stress.

I. INTRODUCTION

MANGANESE sulfide inclusions appear regularly as a constituent of structural steels as determined by the sulfur content. The MnS inclusions improve the machinability of the material due to their beneficial influence on chip embrittlement, tool protection, and flow zone improvements.[1] Although the influence of MnS on machinability is appreciated, the amount, shape, size, and distribution of these inclusions are subject to restrictions. This occurs because the sulfides can act detrimentally on the mechanical properties of the material.[2]

The MnS shows a hardness of 170 HV at room temperature and its Young's modulus ranges between 70 and 140 GPa.[3] Different from most other nonmetallic inclusions, MnS has the property to be softer than the steel matrix during hot working operations.[1] This results in deformation of the originally equiaxed MnS inclusions to flattened shape upon a hot rolling operation. The consequences of pancake or discoid shapes are high stress concentrations on the sharp edges of the deformed MnS inclusions and therewith strong mechanical anisotropy.[4]

Anisotropy in the mechanical behavior of forged components can be experienced, *e.g.*, in ductility, yield strength, and tensile strength, but also in fatigue properties. For instance, the tensile strength of a material is lower when inclusions are oriented transversally to the principal stress as compared with material with longitudinally oriented inclusions.[5] Also, the fatigue strength properties show distinct anisotropy depending on inclusion orientation.[2]

An inclusion that cannot maintain bonding to the matrix will act as a crack within the matrix material.[6,7] It is therefore the aim of the present investigation to evaluate the bond strength between MnS inclusions and the surrounding steel matrix in order to draw conclusions on inclusion behavior in stressed materials.

II. EXPERIMENTAL

Tensile deformation of miniature tensile specimens has been carried out in a tensile stage mounted in the specimen chamber within a scanning electron microscope (SEM).

A. *Material*

As a test material, a medium carbon steel of grade 42CrMo4 (EN 10083-1) (Table I) was used. The steel was melted and cast in vacuum in experimental amounts with tight requirements regarding cleanness. Ingot casting was used in order to avoid initially textured material as often experienced in continuous casting. Deformation and therewith orientation of the material was introduced by a hot cross rolling operation. Rolling deformation occurred along longitudinal (L) and transverse (T) directions with a reduction ratio of 4.5 in the short transverse (S) direction. This hot working operation was carried out at 1200 °C and should create in-plane rotational symmetry of the MnS inclusions. The original shape of the MnS was rated as mainly type II (dendritic appearance) according to the classification of Sims and Dahle.[8] Subsequent through hardening and tempering were performed to a final hardness level of 450 HV30 corresponding to yield and ultimate tensile

S. B. HOSSEINI, Failure Analyst, Researcher, C. TEMMEL, Researcher, and N.-G. INGESTEN, Manager Forged Materials, are with the Materials Technology, Volvo Powertrain Sweden, SE-405 08, Gothenburg, Sweden. B. KARLSSON, Professor, is with the Department of Materials and Manufacturing Technology, Chalmers University of Technology, SE-412 96, Gothenburg, Sweden. Contact e-mail: seyed.hosseini@comhem.se

Table I. Chemical Composition (In Weight Percent) of the Material after Hot Rolling

Material/Elements	S	C	Si	Mn	Cr	Mo	P	N	Sn	Al	V	Cu
42CrMo4	0.045	0.42	0.25	0.76	1.06	0.23	0.003	0.003	0.002	0.005	0.004	0. 01

Table II. Static Mechanical Properties of the Test Material in the L and S Directions; Tensile Values for the L Direction are an Average of the Results from Three 80-mm Tensile Specimens; the Values for the S Direction are Collected from the Miniature (30 mm) Tensile Tests Carried Out in the SEM

Specimen	R_m (MPa)	$R_{p0.2}$ (MPa)	A_5 (Pct)	Z (Pct)	E (GPa)
80-mm test specimens—L	1559	1412	5.89	23	193.5
Miniature test specimens—S	1600	1400	—	—	—

strengths in the longitudinal specimen of 1412 and 1559 MPa, respectively.[2] Tensile values for the S direction were collected from the miniature tensile tests carried out in the SEM (Table II).[9,10] A detailed microstructural investigation and an extensive study on the anisotropic fatigue strength of this material have been carried out by Temmel et al.[2]

For easy understanding, the following notations are used throughout the text: longitudinal direction (L), transverse direction (T), and short transverse direction (S).

B. Specimen Preparation

Miniature tensile specimens were cut out of the rolled, unhardened test material along two orientations in order to get the MnS inclusions aligned with and perpendicular to the specimen axis (Figure 1). The microstructure with the oriented MnS of the original test material is shown in Figure 2.

The miniature specimens were hardened and tempered to a hardness level of 450 HV30, as mentioned previously. Thus, austenitizing was performed at 850 °C, followed by quenching in oil at 120 °C and tempering at 400 °C for 1 hour. This resulted in a martensitic microstructure with previous austenite grain size of typically 25 μm, preventing intergranular cracking during tensile deformation.

The tensile specimens were polished in several passes using cloth and diamond paste suspensions with particles of 6, 3, and 1 μm in size. No further treatments other than demagnetization were performed prior to the investigations in the SEM.

C. Tensile Straining

In-situ tensile testing in an SEM was performed in order to investigate the bond strength between the MnS inclusions and the surrounding matrix. The straining was carried out on a Raith tensile stage, which was mounted in the SEM (Zeiss DSM 940 A, Germany). The specimens were pulled until fracture. The load capacity of the stage was 5 kN, and the crosshead velocity was set to render a strain rate in the waist of the specimens to approximately 10^{-4} s^{-1}. The load cell was calibrated with dummy specimens prior to the tests.[9] During the tests, a prestrain load of 40 N was applied.

D. Microscopy of Deformed Materials

During straining, the test specimens were monitored with the SEM. Images of predefined MnS inclusions were taken at each 12.5 or 25 MPa stress increment, depending on the necessary resolution of the test result. This means that the deformation and cracking of the inclusions could be followed progressively up to the point of final global fracture.

After the tensile deformation, the specimens were further investigated by optical microscopy and an SEM. Examinations were carried out on the fracture surface as
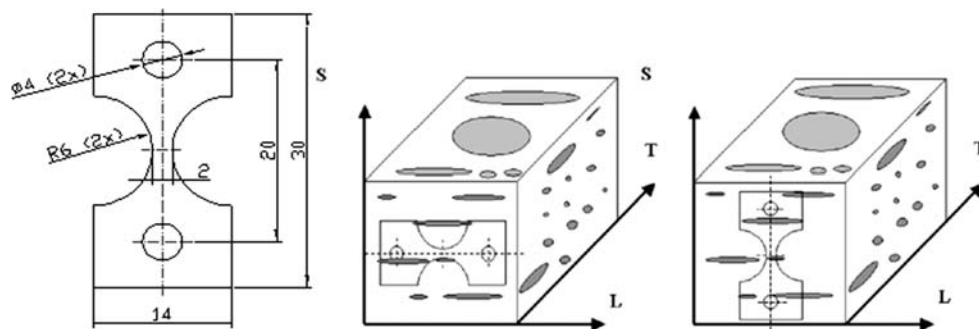

Fig. 1—Miniature tensile test specimen (all dimensions are in millimeters) with a thickness of 1 mm (left). Two different orientations are distinguished (right): L and S directions. (The size and amount of the MnS inclusions in the figure are exaggerated.)
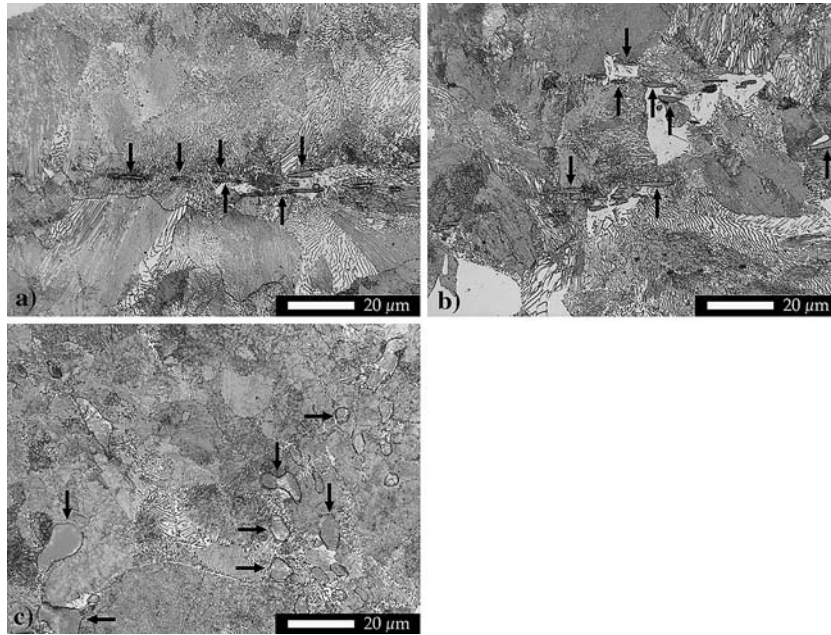
Fig. 2—Original ferritic pearlitic microstructure in the (a) L, (b) T, and (c) S directions. The arrows indicate the position of the MnS inclusions. Images are taken before hardening.

well as on the external and internal surfaces of the tensile bar. Internal surfaces were produced by vertical sectioning through the fracture surface.

III. RESULTS

A. Tensile Test

The tensile testing included six miniature specimens in total, of which three were in the L (L1, L2, and L3) and three in the S (S1, S2, and S3) directions (Figure 3). All stresses are given here as nominal engineering stress, referred to the thinnest waist section. Elongation values were used instead of strain values, because the latter ones are less well defined owing to the gradual change of cross section of the tensile specimens (Figure 1). Further, the recorded load data were estimated to have an inaccuracy of some 8 pct of the displayed values, mainly caused by play in the tensile equipment. Such deficiencies are thought to have much less influence on the stress data.

At first sight, all specimens showed similar behavior up to the region of the yielding at approximately 1400 MPa. However, above this stress level, the longitudinal specimens showed more ductility than the transverse specimens. Also, the fracture stress is noticeably higher for the longitudinal specimens, which fractured at approximately 1700 MPa as compared with only approximately 1600 MPa for the short transverse specimens. Careful observation of Figure 3 reveals also a somewhat steeper slope for the longitudinal specimens, indicating a higher stiffness for the material when MnSs are aligned with the applied stress. The difference in stiffness was estimated to be approximately 7 pct.
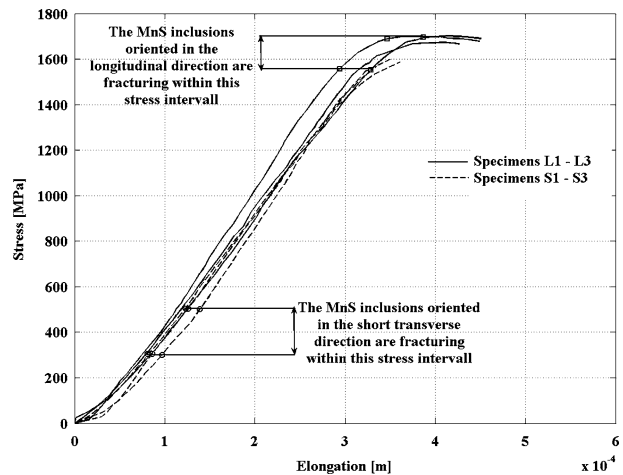

Fig. 3—Tensile test results for specimens L1, L2, L3, S1, S2, and S3. The x-axis shows the elongation between the grips, whereas the y-axis shows the applied nominal stress. Both the elongation and the stress values are the displayed values from the tensile stage controller. The graph has been slightly modified in order to compensate for differences during sample pretensioning.

A major distinction between longitudinal and short transverse specimens is the bonding behavior of the manganese sulfides with the surrounding matrix. In the L direction, the MnS inclusions started to fracture above the initial yielding at approximately 90 pct (1500 MPa) of the global fracture stress. In contrast, in the S direction, the MnS inclusions began debonding from the matrix when only approximately 20 pct of the fracture stress of the material was reached (300 to 500 MPa).
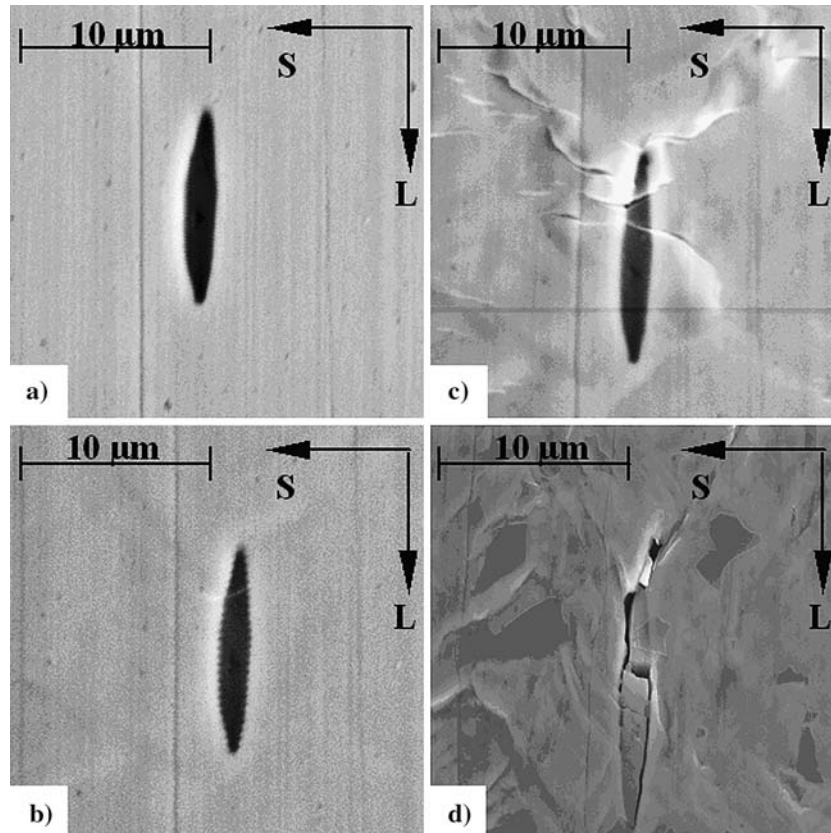
Fig. 4—SEM images of a studied MnS inclusion with the applied load parallel to the L direction: (*a*) the applied stress is 20 MPa, (*b*) the first crack is initiated at the applied stress of 1631 MPa, (*c*) the applied stress is 1698 MPa, and (*d*) unloaded condition.

1. *Longitudinal test*

In the longitudinal specimen L1 (Figure 4), with MnSs aligned with the applied load, the first crack of a selected, typical inclusion initiated at a displayed nominal stress of 1631 MPa (Figure 4(b)) at the interface inclusion–matrix. Consecutively, the crack propagated through the MnS and divided the inclusion into two parts at a stress of 1676 MPa. Several cracks appeared but no debonding was visible at the interface inclusion–matrix (Figure 4(c)). The entire material started to collapse when increasing the stress to 1700 MPa. However, after unloading, the sulfide divided into several parts and it was also debonded from the matrix (Figure 4(d)).

2. *Short transverse test*

In the short transverse test S3 (Figure 5), with extended MnSs perpendicular to the applied load, the MnS inclusions start to debond from the matrix at a displayed nominal stress of only approximately 400 MPa (Figure 5(b)). It should be noted that the large sulfide in Figure 5 is affected by debonding, whereas the small MnS inclusion is not. With increasing stress, the displacement of the inclusion from the matrix strives to a maximum (Figure 5(c)), to relax back after unloading due to specimen failure. However, the detachment of the matrix remains (Figure 5(d)).

3. *Stress-cracking sequences*

Video sequences of the cracking and delamination of the MnS inclusions shown in Figures 4 and 5 are available at the Chalmers University of Technology website[11] under *http://www.chalmers.se/mmt/SV/forsk ning/materialteknologi/projekt/publikation-av-s-b*

B. *Analysis of Internal and External MnS*

Only a fraction of all MnS inclusions fractured or debonded, as can be learned from Figure 6. It became obvious that the size of any individual sulfide plays a role for its behavior. The investigated MnSs of Figures 4 and 5 had a length of 10 to 15 μm. The MnS inclusions of especially that size or larger were susceptible to debonding. However, only about 10 pct of the entire MnS population reached or succeeded such a length. The average length of the sulfide inclusions in the test material was, according to ASTM E 1245–03, determined to be 4.8 μm.[2]

Manganese sulfides were analyzed both internally and externally on the fractured tensile test specimen. Sulfides up to a distance of 2 mm from the fracture surface were investigated. The internal examination was performed on a polished longitudinal cross section of the tensile test bar at a depth of 0.5 mm from the outer surface, while the external study was done on the free surface.
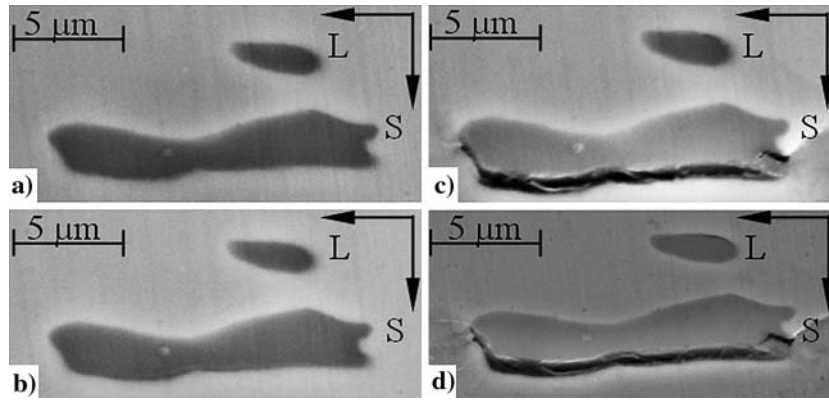
Fig. 5—SEM images of studied MnS inclusions with the applied load in the S direction: (*a*) the applied stress is 20 MPa, (*b*) the large MnS inclusion starts to detach from the matrix at the applied stress of 402 MPa, (*c*) the inclusion continues to separate from the matrix as the stress increases to 1586 MPa, and (*d*) unloaded condition.
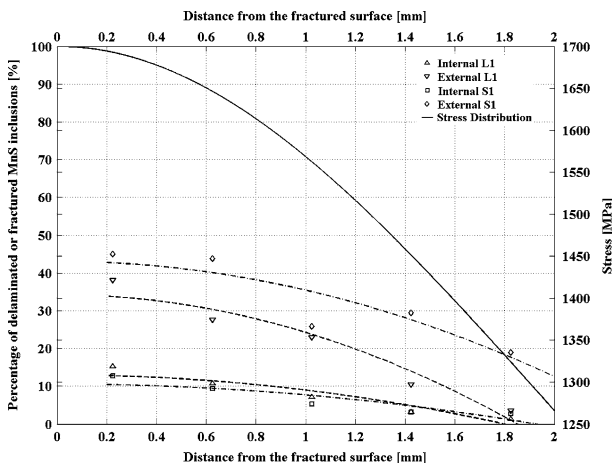

Fig. 6—External and internal analysis of a longitudinal specimen (L1) and a short transverse specimen (S1). For the longitudinal specimen, the sulfide fractures have been counted, whereas for the short transverse specimen, debonded MnS were registered.

Both sample orientations have been scrutinized where sulfide fractures were counted in the longitudinal specimen (L1) and sulfide debondings in the short transverse specimen (S1). These results are presented in Figure 6. The graph shows the portion of fractured or debonded MnS inclusions as a function of their distance from the fracture surface. The count comprises all manganese sulfides, regardless of their size. As mentioned previously, only larger MnS seemed to be vulnerable to either cracking or debonding. However, the critical size of the sulfides increases with decreasing stress. The local principal stress decreases with distance from the fracture surface according to the specimen geometry, resulting in smaller frequency of sulfide fracture or debonding (compare with Figure 6).

For both specimens, failures of MnS occur more readily at the free surface of the specimens, whereas failures are compressed in the bulk material.

IV. DISCUSSION

The studies in SEM revealed different material behaviors depending on the test orientation of the specimen. Differences between the longitudinal and the short transverse deformation character could be seen predominantly in the ductility.

A. *Ductility*

A difference in ductility between the two test series was the extent of a plastic strain of about 0.2 pct preceding fracture for the longitudinal specimens, while the short transverse specimens behaved in a brittle manner once the yield stress level was reached. That ductility difference implies that void nucleation and void growth around inclusions influence the overall ductility. Roberts *et al.*[12] stated that there is a relationship between the ductility of a material and the void nucleation and void growth around deformed flattened inclusions embedded in the material.

In the longitudinal specimens, the inclusion failures occurred either by particle cracking or fragmentation at high stresses followed by decohesion from the matrix after cracking (Figure 4). Similar behavior was observed by Beremin.[13] The debonding of MnS inclusions from the matrix already at low stresses in the short transverse specimens (Figure 5) was also noted by Roberts *et al.*[12] Beremin[13] presents values for inclusion break in the L direction at 1120 ± 60 MPa and inclusion debonding in the S direction at 810 ± 50 MPa. However, those values were derived from investigations on unloaded cross sections of tensile test bars.

In the stressed test materials, numerous voids around manganese sulfides developed. Those voids were more frequent and larger in dimension in the short transverse specimens. According to Benzerga *et al.*,[14] the ductility in short transverse specimens is limited by the coalescence of elongated cavities. Much further research has been done in this field. Speich and Spitzig,[15] for instance, present their results on changes in, *e.g.*, tensile
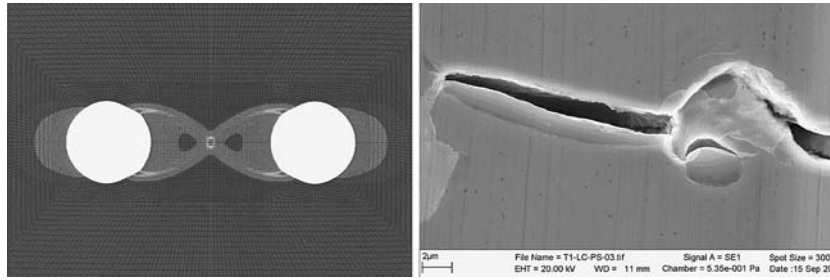
Fig. 7—Finite element simulation showing strain bands between two circular MnS inclusions (Karttunen,[10] left). Several MnS inclusions were linked along strain bands in the present investigation (test S1, Hosseini,[9] right). Loading direction vertically.

ductility in a study on AISI 4340 steel with different sulfur contents.

B. *Creation of Strain Bands Due to MnS Inclusions*

It has been discussed whether the spacing and the shape of the inclusions influence the ductility of the material. Strain bands form between inclusions at higher stress levels. Depending on the distance between the inclusions, interlinking of voids at debonded inclusions can occur (Figure 7). According to Karttunen,[10] the spacing between inclusions has a great influence on the formation of the strain bands and therewith the interlinking of voids. That might explain the diversities in mechanical behavior experienced between L and S test directions, where inclusions appear differently.

C. *Mechanisms for Delamination and Cracking*

Elongated inclusions aligned (longitudinal) with the tensile axis show a strong propensity to fracture, whereas inclusions perpendicular (short transverse) to the principal stress tend to debond from the surrounding matrix material. This occurs because, when a stressed elongated sulfide inclusion is in line with the tensile force, the surrounding matrix tends to compress the MnS inclusions and thus maintains the bond as long as the tensile load is applied (Figure 8, left). On the other hand, a stressed elongated inclusion oriented perpendicular to the direction of principle stress at the interface between the MnS inclusions and the matrix shows the tendency to separate (Figure 8, right). According to Leslie,[16] void formation at an inclusion arises due to tensile stresses normal to the interface sufficient to create debonding.
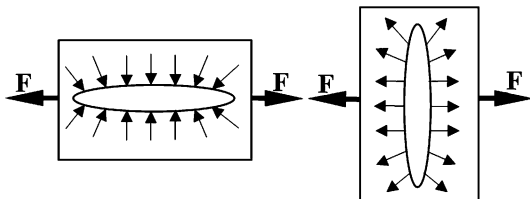

Fig. 8—Elongated MnS inclusion directed parallel to (left) and perpendicular to (right) the tensile force.

The most important consequence of the two mechanisms for longitudinal and short transverse orientation of the sulfide inclusions is the necessary stress level for void formation at MnS inclusions (Figure 3). In the L direction, cracks do not develop until stress levels of approximately 1600 MPa in the plastic regime of the material. Naturally, the length of those cracks equals at first the thickness of the inclusions. However, in the S direction, the MnS inclusions detach from the surrounding matrix at a stress level of only approximately 400 MPa. The length of those cracks is, accordingly, equal to approximately the length of the inclusions, which in most cases is much larger than the cracks present in the L direction (compare the length of the cracks in Figures 9 and 10, right).

Longer cracks arising at remarkably lower stress levels, as for the short transverse material, form a much more severe situation at the crack tips. This ultimately influences the overall mechanical properties of the material. Further, the two different mechanisms of void formation around elongated inclusions imply that the material might be vulnerable to mechanical anisotropy. Indeed, Temmel et al.[2] showed that fatigue anisotropy increases in forged material when flattened, oriented MnS are present. The increase of anisotropy could be attributed to the MnS population.

Inclusions both at free surfaces but also internally follow the described failure mechanisms. However, for both orientations, void development around inclusions and inclusion fractures are notably more frequent at the free surface of the test bar as compared with internal sections (Figure 6). This accords with the results of Roberts et al.,[12] who showed that the critical strain for void formation at the free surface is an order of magnitude smaller than the strain necessary for void formation at internal inclusions. This implies that less energy is necessary to create a void at an inclusion at a free surface, which is plausible.

Inclusions contained in the short transverse specimens debond at their interface from the matrix material. As already observed by Roberts et al.,[12] the bond at some internal inclusions might open locally along the interface rather than forming single, large delaminations at the inclusion surface. Those small voids often link to form larger cavities at increased stresses. Such behavior of the inclusion-matrix bond was detected in the present study (Figure 10, left). By contrast, cavities at the free surface of the specimen always formed around an inclusion
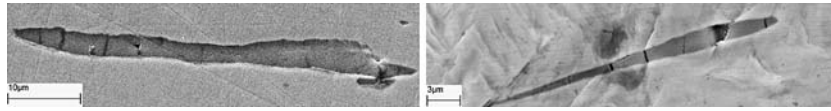
Fig. 9—MnS inclusion in the interior with a length of 50 μm (left) and a MnS inclusion at the free surface with a length of 25 μm (right) both contain several cracks. The load is aligned parallel to the elongated MnS inclusion. Inclusions from the broken test bar (L1).
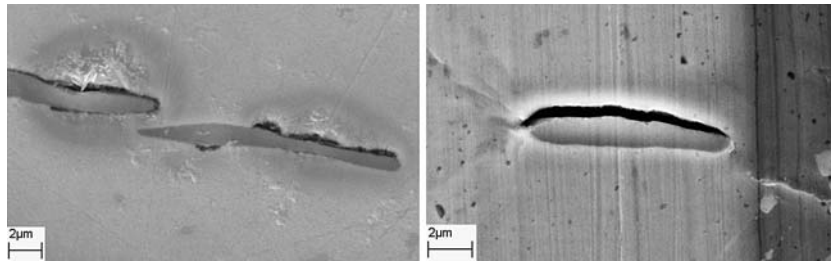

Fig. 10—Void development around a single MnS inclusion in short transverse specimen (S1). Several voids have formed and linked to a rather large crack, and the inclusion has partly separated from the matrix (left). The MnS inclusion at the polished free surface (right) has separated from the surrounding matrix, thus forming a crack. The principal stress is perpendicular to the elongated MnS inclusions. Inclusions from a broken test bar (S1).

initially as a single large void. Yet, also internally, some cavities formed as single large delaminations along the entire length of the interface.

It seems that the surface at the internal section has been affected by the polishing solution during the specimen preparation. It is believed that the solution together with the sulfur of the MnS can form sulfuric acid, which consequently may etch away matrix material especially at the inclusion-matrix interface. Local acid attack around internal inclusions can therefore occasionally be misinterpreted as local void formation due to material stressing.

V. CONCLUSIONS

The bond strength between MnS inclusions and the matrix has been investigated in strained material. The orientation with respect to MnS inclusions had an essential role during the tensile deformation, where material with sulfides oriented parallel (longitudinal specimens) and perpendicular (short transverse specimens) to the nominal stress was investigated. The material used was a medium carbon steel (42CrMo4) with a sulfur content of 0.042 wt pct. The material was hot cross rolled with a reduction ratio of 4.5. This reduction led to oriented, flattened MnS inclusions. Subsequent hardening and tempering was performed to reach a hardness of 450 HV30.

The deformation characteristics for the two directions can be summarized in the following manner.

Longitudinal specimens:

1. The MnS inclusions fracture into several parts at a nominal stress of approximately 1600 MPa. That stress level corresponds to about 90 pct of the nominal fracture stress.
2. The MnS inclusions debond from the matrix after cracking has taken place. Debonding can be asserted only after unloading.

Short transverse specimens:

1. The MnS inclusions debond from the matrix. No fractures of MnS could be observed.
2. Debonding between the inclusion and the matrix occurs at stresses of approximately 400 MPa, corresponding to roughly 20 pct of the nominal fracture stress.
3. Tensile test bars in the S direction exhibit a less ductile behavior than the longitudinal bars.

Oriented MnS inclusions lead to anisotropic material behavior. In order to be able to diminish the effect of deformed inclusions on anisotropy, the shape, size, and distribution of the inclusions have to be controlled.

The behavior of the inclusions at a free surface and within the material is rather similar. However, for both specimens, void formation at MnS inclusions occurs more readily at the specimen free surface compared with the condition in the bulk material.

ELECTRONIC SUPPLEMENTARY MATERIAL

The online version of this article (doi:10.1007/s11661-007-9122-9) contains supplementary material, which is available to authorized users.

REFERENCES

1. R. Kiessling and N. Lange: *Non-Metallic Inclusions in Steel (Parts-IV)*, 2nd ed., The Metals Society, London, 1978, pp. 60, 104, 118, and 162.

2. C. Temmel, B. Karlsson, and N.-G. Ingesten: *Metall. Mater. Trans. A*, 2006, vol. 37A, pp. 2995–3007.
3. D. Brooksbank and K.W. Andrews: *J. Iron Steel Inst.*, 1972, vol. 210, pp. 246–55.
4. C. Kaynak, A. Ankara, and T.J. Baker: *Mater. Sci. Technol. (UK)*, 1996, vol. 12, pp. 557–62.
5. *ASM Handbook*, vol. 10, *Failure Analysis Prevention*, 8th ed., ASM INTERNATIONAL, Metals Park, OH, 1975, pp. 291–95.
6. Y. Murakami: *Metal Fatigue: Effects of Small Defects and Nonmetallic Inclusions*, Elsevier, Amsterdam, 2002, p. 369.
7. S. Suresh: *Fatigue of Materials*, 2nd ed., Cambridge University Press, Cambridge, USA, 2004, p. 679.
8. C.E. Sims and F.B. Dahle: *Am. Foundrymen's Assoc., Trans.*, 1938, vol. 46, pp. 65–132.
9. S.B. Hosseini: *Bonding between MnS Inclusions and the Steel Matrix*, Chalmers University of Technology, Göteborg, Sweden, 2005.
10. K. Karttunen: *Numerical Investigation of Ductile Fracture Induced by MnS Inclusions*, Chalmers University of Technology, Göteborg, Sweden, 2005.
11. http://www.chalmers.se/mmt/SV/forskning/materialteknologi/projekt/publikation-av-s-b.
12. W. Roberts, B. Lehtinen, and K.E. Easterling: *Acta Metall.*, 1976, vol. 24, pp. 745–58.
13. F. Beremin: *Metall. Trans. A*, 1981, vol. 12A, p. 723.
14. A.A. Benzegra, J. Besson, and A. Pineau: *Acta Mater. Inc.*, 2004, vol. 52, pp. 4623–38.
15. G.R. Speich and W.A. Spitzig: *Metall. Trans. A*, 1982, vol. 13A, pp. 2239–58.
16. W.C. Leslie: *ISS Trans.*, 1983, vol. 2, pp. 1–24.